35th Annual International Conference of the IEEE EMBS
Osaka, Japan, 3 - 7 July, 2013

A Novel Endoscopic Spectral Imaging Platform Integrating K-Means Clustering for Early and non-Invasive Diagnosis of Endometrial Pathology

Vasileios Kavvadias, George Epitropou, Nikos Georgiou, Fani Grozou, Minas Paschopoulos and Costas Balas, *Member, IEEE**

Abstract— **We report a multimodal endoscopic system capable of performing both color and fast multispectral imaging in the spectral range 400-1000nm. The system is based on a computer controllable tunable light source, which can be coupled with all types of endoscopes. Performance evaluation showed about 60% flat transmittance in almost all the operating wavelengths, at about 13 nm bandwidth per tuning step. With this system adapted to a thin hysteroscope, we also report, for the first time, spectral analysis of the endometrium and unsupervised/objective clustering of the spectra. We have implemented a method combining the k-means algorithm with the silhouette criterion for estimating the number of the distinguishable spectral classes that may correspond to different medical conditions of the tissue. It was found that there are five-well defined clusters of spectra, while preliminary clinical data seem to correlate well with the tissue pathology.**

I. Introduction

After several decades of technology and application development, endoscopy has been established as an indispensible diagnostic tool to a variety of internal medicine fields. However it has been widely recognized that there is significant room for improvement mainly through the merging of endoscopy with novel and advanced optical imaging methods and technologies. These include confocal imaging (CI), optical coherence tomography (OCT) and spectral imaging (SI) [1]. CI and OCT with or without contrast enhancing agents, provide histological information *in vivo* for the very small tissue area. Spectral imaging provides, in principle, information for a much larger tissue area, which is essential in the clinical practice. Integrated to endoscopy, this imaging modality provides enhanced visualization of several invisible features of diagnostic importance.

There has been a considerable effort towards the integration of general purpose tunable filter technologies for enabling endoscopic spectral imaging. These include revolving discrete filter arrangements known as Narrow Band Imaging (NBI), liquid crystal tunable filters (LCTFs), acousto-optical tunable filters (AOTFs) and Michelson interferometers [2]. Although the last three approaches can provide complete spectrum, they suffer from several limitations, which make them suboptimal solutions for endoscopy. Particularly, LCTFs are polarization dependent electro-optic devices with a poor light throughput being approximately 30%. AOTFs produce blurry images due to second order harmonics from the acoustic driver. The operating wavelength range of both AOTFs and LCTFs is limited to either the visible or to the Near-Infrared (NIR) spectral range, requiring the interchange of different modules if one wants to cover the entire sensitivity spectral range of the silicon based imaging sensors (CCD and CMOS). Additionally, the full width half maximum (FWHM) of these tunable filters varies significantly together with the light throughput across the operating wavelength range, which makes their calibration cumbersome. These technical shortcomings of tunable filter technologies together with their relatively high cost comprise a barrier to their adoption in the clinical research and diagnosis. This barrier becomes even higher when their integration to endoscopy is attempted with the main problems, being the very low light throughput of endoscopes and especially of the thin ones (2-4 mm). For this reason, simplified and rather trivial solutions have been employed instead, which allows for only a partial exploitation of the diagnostic potential of SI. The basic representative of this class of instruments is the NBI endoscopy. NBI was developed primarily for enhancing the visualization of mucosal microvasculature and to identify vascular alterations indicative of pathologic conditions [3]. It is based on the simple interchange of two (415nm, 540nm) or three band-pass filters in front of a white-light source, which is coupled with the illumination path of the endoscope. This discrete, band-pass light-filtering arrangement produces a higher contrast between vascular structures and the surrounding mucosa [4]. Higher contrast is obtained by exploiting the existing light-absorption differences between these tissues, which are maximized within predetermined wavelength ranges. However, the provided enhancement, although useful is some cases, it is of limited diagnostic importance. This is because the development of consensus regarding the predictive value of the various vascular patterns is still pending [5]. The collection of a full spectral cube remains much more valuable than simply inspecting discreet spectral bands. Two-dimensional spectroscopy can provide NBI and on top of it "spectral signatures" of tissue lesions. The latter correspond to quantitative information with regard to biochemical and structural changes associated with several clinical conditions. This would enable the non- invasive,

*V. Kavvadias, G. Epitropou, N. Georgiou, and C. Balas are with the Department of Electronic and Computer Engineering, Technical University of Crete, Chania 73100, Crete, Greece (corresponding author to provide phone: +30-28210-37223; email: balas@electronics.tuc.gr).

M. Paschopoulos and F. Grozou are with the Department of Obstetrics and Gynecology, Ioannina University Hospital, Ioannina 45110, Greece (email: mpasxop@ccuoi.gr).

early detection and grading, while, at the same time, providing guidance for biopsy sampling, surgical treatment and follow up.

In an attempt to address this demand we present in this report an affordable, high-throughput and fast SI system that can be integrated to existing endoscopic workstations without changing significantly routine practices. This is because it provides both live color imaging and pixel by pixel spectral analysis. The system has been successfully adapted to a thin (3.5 mm) endoscope, which was used for inspecting the endometrium (hysteroscope). We also report our findings from the spectral measurement and analysis of the endometrium, which, to the best of our knowledge, are both presented for the first time. Particularly, the obtained millions of spectra were automatically clustered on the basis of their distinct spectral characteristics. This process revealed objectively that there are 5 to 6 distinguishable spectral clusters that may correspond to different medical conditions. The pilot clinical use of developed "Spectral Clustering" (SpeCL) endoscope in identifying and mapping pathologic conditions of the endometrium are finally presented and discussed.

II. Materials and Methods

A. SPECL System Design and Set-Up

The SPECL hardware design was based upon a tunable wavelength light source and a camera operating in both color and monochrome modes. The tunable light source was build around a variable optical filter (VOF), which has the property of transmitting a narrow spectral band of the incident light while all the other frequencies are blocked. The center wavelength of the transmitted band changes continuously along its longitudinal axis and therefore it can act as a tunable filter when it is translated along this axis in front of a focused light source.

The VOF operates in the spectral range 400-1000nm (Schott Veril) covering both the visible and the NIR bands. It is quite convenient that this wavelength range matches the sensitivity range of the silicon-based imaging sensors. As discussed in the introduction, the wide operation spectral range of VOF improves its competiveness as compared with the AOTFs and LCTF. Fig. 1 illustrates the block diagram of the SPECL endoscope. The VOF was mounted onto a motorized linear translation stage with about 160 mm stroke. A unipolar stepper motor was used, which is a robust closed loop control system for ensuring high positioning accuracy. The linear motion of the filter is controlled with the aid of an in-house built electronic unit, which is interfaced with a consumer class personal computer (Intel i5 processor, 2.5 GHz, 6 GB RAM) via USB 2.0 port. The unit has been built around the AT mega 162 (Atmel), microcontroller. The light source is a Xenon bulb (150 W), which is focused onto the VOF's surface with the aid of a parabolic mirror. An electronically controllable mechanical iris and a cold mirror system are interposed in the light path, both filtering the beam before it reaches the VOF. This is done for minimizing the risk of thermal damaging. Actually, the dichroic mirror system combines two dichroic mirrors placed between the

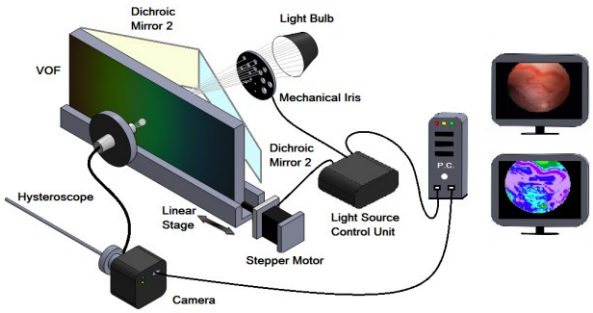

Figure 1. The block diagram of the spectral clustering endoscope.

VOF and the iris, each one forming approximately at 45° angle with the VOF. The first dichroic mirror (Thorlabs DMSP805R), which transmits >90% in the spectral range 380-790nm and reflects > 90% in the spectral range 820-1300nm was used to "cover" UV-visible part of the VOF. The second dichroic mirror (Thorlabs DMSP 1000R), transmits >90% in the spectral range 520-985nm and reflects > 90% in the spectral range 1020-1550 nm and it was used for protecting the red-NIR part of the VOF. The mirror set is moved together with the VOF and ensures that a great amount of the out of band energy of the light source is rejected (reflected), while at the same time the transmitted in band energy to the VOF remains substantially unchanged. The filter is removed away from the light spot when the user selects to switch the system to the color imaging mode. In this way, when the SPECL system operates in the color imaging mode, the VOF is cooled down to ambient temperatures. A color camera (Sony ICX674) with its IR-cut filter removed, is used for capturing both color and monochrome (visible and NIR) spectral images. The role of the camera's IR-cut filter in ensuring correct, IR-free color reproduction and imaging is substituted by the extending part of first dichroic mirror, in the right side of the VOF (fig 1). Switching between spectral and color imaging is performed rapidly, through computer control, which toggles the camera's output between the monochrome/color states. It also rotates the multihole-type iris so that more light passed through the iris holes when it is switched to operate in the SI mode.

B. SPECL System Operation-Spectral and Color Image Acquisition

Before acquiring spectral or color images, the SPECL system is calibrated. Calibration refers to both color and spectral imaging and it is performed by utilizing a reference sample with unity reflectance across the entire 400-1000nm spectral range. The system scans the sample step by step and the gray values of the sample serve as a feedback for the system to automatically regulate the sensor's exposure time and/or the light source's iris. Calibration process ends when the gray values reach a certain value for all spectral bands. When the user activates e.g. the spectral imaging procedure the VOF is moved to the corresponding position and the camera captures the image in a synchronized manner. Then, the filter is moved to the next position and the procedure continues until the entire set of the predetermined set of images is collected. Image capturing is performed with the

exposure/iris settings as they have been determined during calibration and have been stored in a look-up-table for every tuning step.

With the SPECL system calibrated and switched to the color imaging mode, the operator inserts the endoscope into the hollow organ, while inspecting a color or a monochrome spectral image onto one of the two monitors of the system. Monochrome spectral image offers a similar to the NBI operations as it can be used for enhancing the observed contrast. The SPECL system integrates a fast spectral scanning procedure which operates as follows: With either real time color or spectral imaging, the operator locates a suspicious area to be analyzed. The system is then switched to the spectral scanning mode and ten seconds are given to the operator and to the patient to prepare and remain still. Next, and within two seconds, fifteen full resolution spectral images and one color image are collected and stored in system's hard drive. Upon completing the scanning procedure, the system switches back automatically to the real time color imaging mode. This stack of images (spectral cube) is then processed for detecting and correcting image misregistration problems and for calculating the cluster map image (CMI), based on the algorithms that will be described below**.** Calculations last for approximately two seconds and upon completing this second task, an artificial image is displayed on the second monitor. Each cluster in this image is represented with an artificial color for facilitating localization and identification of abnormal areas.

C. Clustering of Spectra Obtained from the Endometrium

The SPECL endoscopic platform was used for examining the inner lining of the uterus, known as endometrium. In fact, the SPECL system enabled for the first time the collection of spectra from the endometrium corresponding to a wide range of clinical conditions. The examination of the endometrium is routinely performed with the aid of a very thin rigid endoscope (3.5 mm diameter), which it is called hysteroscope. Hysteroscopy is performed for a variety of gynecological conditions, such as abnormal uterine bleeding (menorrhagia), infertility, polyps, fibroids, endometrial adhesions, uterine diaphragm, endometrial hyperplasia, cancer etc.

Although endometrial abnormalities are manifold that may be the etiology of several conditions ranging from infertility to cancer, all the existing diagnostic tests including transvaginal ultrasonography, sonohysterography and diagnostic hysteroscopy, have been proved to be just moderately accurate in detecting intrauterine pathology [6],[7]. Very recently and in an attempt to improve the diagnostic performance of hysteroscopy, the NBI endoscopy technique has been used in examining the endometrium but with the limitations outlined in introduction [8].

The SPECL system was installed in the outpatient clinic of the Obstetrics and Gynecology department of the University of Ioannina, Ioannina, Greece. The SPECL's camera and tunable light source was coupled with a 3.5 mm Bettochi Hopkins II hysteroscope (Karl Storz). A clinical study is currently underway with the purpose of establishing the spectral patterns of various pathologic conditions of the endometrium. The participants of the study are examined with the SPECL endoscope following the standard endoscopic procedures and guidelines. All women participating to the study have signed an informed consent and the ethics committee of the hospital has approved the study. During the preliminary phase of this large study, data were obtained from fifteen cases with different conditions (normal and pathologic). Particularly, these cases span a wide spectrum ofconditions including: 3 normal, 2 polyps, 1 inflammation, 2 abnormal uterine bleeding, 5 endometrial hyperplasia and 2 cancer (biopsy confirmed). By following the procedures described in paragraph II.B, 25 spectral cubes were collected from all these cases using the SPECL system.

It is easy to realize that it is impossible to visually analyze this huge number of spectra (2 million per spectral cube) and to come up with a realistic estimation of the number of the distinguishable spectral classes that might correlate with the normal/pathologic conditions of the endometrium. However the objective estimation of the number of the spectral classes is of key importance for performing spectral or (eventually) pathology clustering. For example, this knowledge is essential when unsupervised classification (e.g. K-means algorithm) is intended to be applied in a data set. This is because the data analyst needs to furnish the algorithm with *a priori* knowledge with regard to the number of the classes. Then the algorithm undertakes the task of partitioning the data within these classes. For the purpose of estimating the number of the spectral clusters and identifying diagnostic content of the corresponding spectral categories we have implemented a methodology based on the combination of the k-means algorithm [2] and automatic clustering evaluation methods. We employed multiple replications of the algorithm with different initial cluster centroid positions for avoiding converging to local minima. Two strategies were tested with similar results, selecting k pixels at random, and performing a preliminary clustering phase on a random 10% subsample of pixels.. The later converge to an optimum set of clusters. The method considers a clustering task satisfactory only when the intra-cluster variance is minimized while at the same time the inter-cluster variance is maximized. Variances are calculated by adopting the cosine similarity metric [9].

The spectral cubes underwent post processing and analysis by employing the k-means algorithm which allows for the unsupervised clustering of the spectra. Initially, k-means clustering of the spectra was performed several times whereas each time a certain number of classes was assumed to exist within the range of 4 to 12 classes ($(4 \le k \le 12)$. This range was hypothesized on the basis of visual examination of representative spectra, collected from each particular clinical case. Next, we employed the Silhouette index [10] for the purpose of precisely and objectively assessing the number of the distinguishable by the system spectral classes. Silhouette index $s(x)$ is given by the following formula:

$$s(x) = \frac{b(x) - a(x)}{\max\{a(x), b(x)\}} \tag{1}$$

where $a(x)$ is called "cohesion" and is the average (similarity) distance of x vector (expressing spectra) with the other vectors within the same cluster and $b(x)$ is the (minimum) average distance of vector x to the vectors of belonging to other clusters.

Apparently, as the difference between these two terms is becoming larger (≥ 0), a better clustering of the data is indicated. More specifically, the mean value over all these normalized differences (Silhouette coefficient) for every pixel in the spectral cube is calculated and the procedure is repeated until all clustering results obtained with different number of k-means input classes were estimated. The estimated number of distinguishable spectral classes belonging to the dataset is suggested by the clustering result with the largest Silhouette coefficient.

III. Results and Discussion

The light throughput of the SPECL's-VOF light source was measured with the photometer (Thorlabs PM100D) and found to increase from 30-60% in the range 400-460 nm and then remained flat for all other wavelengths within the visible and the infrared wavelength range. The FWHM of the SPECL's-VOF light source was measured with the spectrometer (Ocean Optics USB4000) and found to range from about 11nm to about 14 nm, indicating a quite sufficient spectral resolution across the operating wavelength range. The combined high and flat light throughput and spectral resolution was the key factor that enabled the SPECL endoscope to perform fast (within 2 s) and of high spatial resolution, imaging. This was obtained even in the case of a 3.5 mm thin, low throughput hysteroscope. Figure 2 illustrates a series of representative spectral images belonging to a spectral cube. In the bottom-right part of the figure the corresponding color image and the calculated spectral clustering map (bottom right) are displayed. As expected, the 440nm image shows superficial blood vessels with high contrast due to the high absorption of oxy-, deoxy-hemoglobin in the vicinity of this band. In the NIR band the blood vessels and the superficial features of the endometrium become transparent, thus allowing for the visualization of underlying features, such as connective tissue (whiter areas). The clustering map shows, with different pseudocolors, 5 to 6 distinguishable spectral classes. It is clearly seen that their spatial heterogeneity can be identified neither in the raw color nor in the spectral images, which indicates the diagnostic value of this artificial image. The number of the different clusters appearing in the clustering map was determined to be 5 to 6 on the basis of the maximization of the Silhouette index. Going one step further, we have attempted to correlate the "colors" of the particular clusters with endometrial tissue conditions, on the basis of the data collected, thus far (spectral cubes and biopsies). Particularly green hues seem to correspond to normal tissue; blue-purple areas indicate the presence of inflammation, while red shows incipient and white-yellow atypical hyperplasia. Interestingly, figure 2 was selected because it shows that all these conditions are possible to coexist at the same tissue area. It is worth noticing that the system has successfully identified five out of the five cases with biopsy confirmed

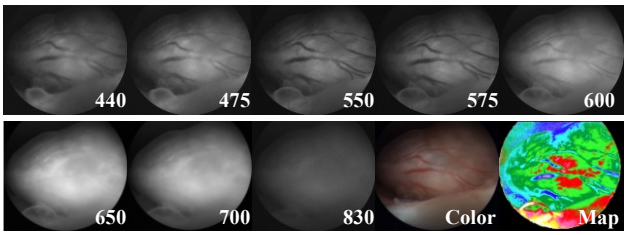

Figure 2. Spectral, color and color-coded images of the endometrium. Different artificial colors correspond to different clusters of spectra and eventually to different medical conditions.

atypical hyperplasia. Despite these very good initial results, a higher confidence, with regard to the SPECL's diagnostic performance, need to be established. Clinical testing of SPECL endoscope is currently underway for establishing sensitivity-specificity statistics in a sufficient number of clinical trial participants, which have been defined with the aid of calculations of statistical power.

IV. Conclusions

We have described a novel spectral clustering endoscope and have identified that in the case of the endometrium there are 5 to 6 distinguishable clusters of spectra. Preliminary clinical validation, currently in progress, shows that the identified clusters of spectra correlate well with tissue pathology. This new technology is therefore of high potential; to provide *in vivo*, early detection, and grading of the lesion, to minimize the need for biopsies, to offer objective follow up, to guide and to evaluate treatments.

References

[1] C. Balas "Review of biomedical optical imaging—a powerful, non-invasive, non-ionizing technology for improving in vivo diagnosis," Meas. Sci. Technol. IoP, vol. 20, no. 10, 2009

[2] C. Balas, G. Epitropou and C. Pappas: "Multi/Hyper-Spectral Imaging," *in Handbook of Biomedical Optics*, Taylor&Francis Books, Inc, USA, 2011

[3] K. Kuznetsov, R. Lambert and J. F. Rey, "Narrow-band imaging: potential and limitations," *Endoscopy*, vol. 38, pp. 76-81, 2006.

[4] I. K. Gono "Multifunctional Endoscopic Imaging System for Support of Early Cancer Diagnosis" *IEEE Journal of Selected Topics in Quantum Electronics*, vol. 14, no. 1, pp 62-69, 2008

[5] L. M. Song, *et al*., "Narrow band imaging and multiband imaging," *Gastrointestinal Endoscopy*, vol. 67, no. 4, pp. 581, 2008.

[6] C. Farquhar, A. Ekeroma, S. Furness and B. Arroll, "A systematic review of transvaginal ultrasonography, sonohysterography and hysteroscopy for the investigation of abnormal uterine bleeding in premenopausal women," *Acta Obstetricia et Gynecologica Scandinavica*, vol. 82, no. 6, pp. 493-504, 2003.

[7] T. J. Clark, *et al*., "Accuracy of hysteroscopy in the diagnosis of endometrial cancer and hyperplasia," *JAMA: The Journal of the American Medical Association*, vol. 288, no. 13, pp. 1610-1621, 2002.

[8] I. Kisu, *et al*., "Narrow band imaging hysteroscopy: a comparative study using randomized video images," *International Journal of Oncology*, vol 39, no. 5, pp. 1057-1062, 2011.

[9] Zhong, Shi. "Efficient online spherical k-means clustering," *Neural Networks, 2005. IJCNN'05*. Proceedings. 2005 IEEE International Joint Conference on. Vol. 5. IEEE, 2005.

[10] N. Bolshakova and F. Azuaje, "Cluster validation techniques for genome expression data," *Signal Processing*, vol. 83, no. 4, pp. 825-833, 2003.